Conformation of Pyrene Labeled Amylose in DMSO Characterized with the Fluorescence Blob Model

Lu Li and Jean Duhamel*

Institute for Polymer Research, Waterloo Institute for Nanotechnology, Department of Chemistry, University of Waterloo, Waterloo, ON N2L 3G1, Canada

* To Whom correspondence should be addressed.

ABSTRACT

Amylose and poly(methyl acrylate) were randomly labeled with pyrene to yield a series of Py-Amylose and Py-PMA constructs and their ability to form excimer in DMSO was characterized quantitatively by steady-state and time-resolved fluorescence. First, the ratio of the fluorescence intensity of the excimer over that of the monomer, namely the I_E/I_M ratio, was obtained from the fluorescence spectra. Second, the product $<k_{blob} \times N_{blob}>$ was obtained from the Fluorescence Blob Model (FBM) analysis of the fluorescence decays. Both I_E/I_M and $<k_{blob} \times N_{blob}>$ yielded similar values when expressed in terms of moles of pyrene per backbone atom for Py-Amylose and Py-PMA. Since I_E/I_M and $<k_{blob} \times N_{blob}>$ reflect the efficiency of pyrene excimer formation, the similar behaviour observed for both parameters obtained for rigid amylose and flexible PMA could only be rationalized by postulating that amylose adopted a compact helical conformation in DMSO. To confirm whether this was possible, molecular mechanics optimizations were conducted with the *HyperChem* program on Py-Amylose assuming a helical conformation for amylose in DMSO. Two pyrene labels were found to overlap properly, and thus form excimer efficiently, if they were separated by no more than 5 anhydroglucose units up and down the amylose helix around the anhydroglucose unit bearing the reference pyrene label. This result suggested that excimer formation would not occur if two pyrene labels were separated by more than 5 + 5 + 1 = 11 anhydroglucose units in perfect agreement with our findings that $<N_{blob}>$ obtained from the FBM analysis of the fluorescence decays acquired with the Py-Amylose solutions in DMSO equaled 11 ± 2. The good agreement between simulations and experiments led to the conclusion that amylose must adopt a helical conformation in DMSO.

INTRODUCTION

The conformations of macromolecules in solution can be grossly divided into two major categories, whether they are flexible (random coil) or rigid (α–helix or β–sheet for polypeptides). In turn, the conformation of a macromolecule in solution will have a major impact on its solution properties. For instance, the viscoelasticity or osmotic pressure of the solution of a macromolecule will be more strongly affected if the macromolecule adopts a more flexible conformation as it is likelier to undergo more pronounced conformational changes upon application of an external shear[1] or addition of a specific chemical like an acid/base[2] or a ligand,[3] an outcome that might be desired or unwanted depending on the application at hand. Consequently, the determination of the conformation of macromolecules in solution has always been of tremendous importance to rationalize their solution properties.

One such macromolecule is amylose which is one of the two main constituents of starch, the other constituent being amylopectin. Amylose is a linear polysaccharide where the anhydroglucose units are linked via α–(1 – 4) linkages (see Figure S1 in Supporting Information (SI)). Water, dimethylsulfoxide (DMSO), and water-DMSO mixtures have been shown to effectively solubilize amylose. In aqueous solutions, optical rotation, intrinsic viscosity, light scattering, and sedimetation measurements have demonstrated that amylose adopts a random coil conformation.[4-6] However, despite much experimental work done on dilute solutions of amylose, its conformation in DMSO is still a matter of controversy. Early work trying to establish a scaling relationship between intrinsic viscosity [η] and weight-average molecular weight (M_w) led to different conclusions. The Flory exponent ν obtained by intrinsic viscosity experiments in DMSO has been reported to equal 0.64,[7] 0.70,[4] 0.87,[8] and 0.91.[9] The first two ν–values were those expected for a

random coil, while the last two results suggested a semirigid and predominantly helical conformation. Some of the above studies have also determined the persistence length of amylose which is a measure of the stiffness of this biopolymer. The persistence length of amylose in DMSO has been reported to equal 2 nm,[10] which is comparable to that of flexible poly(methyl methacrylate), or 9 nm,[9] which oppositely suggests a stiff biopolymer. The difference in interpretation is probably rooted in the experimental difficulty of accurately determining M_w for amylose samples as well as the weak dependence of the intrinsic viscosity on molecular weight for shorter polysacharides.[10]

On the other hand, a conformational transition from a coil to an helix induced by changes in solvent conditions has been detected by NMR,[11,12] specific optical rotation,[13] and intrinsic viscosity.[7] The ^{1}H NMR spectra of amylose in DMSO-d_6 at elevated temperature showed an upfield shift of the hydroxyl proton signals. This observation was taken as evidence that the intramolecular hydrogen bonds necessary for amylose to form a helical structure were severed at high temperature.[12] Another study based on specific optical rotation showed that addition of tetramethylurea decreased the specific optical rotation of amylose in DMSO. This result suggested that the numerous cooperative intramolecular hydrogen bonds necessary to maintain amylose in a helical conformation were disrupted by the addition of urea.[11] While informative about a possible change in amylose conformation, the above studies were aimed to detect the conformational transitions induced by a change in solvent conditions rather than characterize the actual conformation of amylose in DMSO. More recently, molecular simulations on 55 amylose segments 55 anhydroglucose units long have showed that the amylose helix is not stable and rapidly denatures into a random coil in DMSO.[14]

As the above discussion made clear, the conformation of amylose in DMSO, being either a random coil or a helix, remains to be determined. Since the two conformations would lead amylose to exhibit very different internal dynamics in solution, pyrene excimer fluorescence was applied to characterize the internal dynamics of amylose in DMSO. Over the past few decades, pyrene-labeled polymers have become instrumental to study how internal chain dynamics in solution are affected by solvent quality,[15 - 20] polymer concentration,[21-23] solution temperature,[24-26] and side chain length[27,28] to name but a few examples. Consequently, amylose was randomly labeled with pyrene to yield Py-Amylose and fluorescence measurements were conducted on the dilute Py-Amylose solutions whose fluorescence decays were analyzed with the Fluorescence Blob Model (FBM). A fluorescence decay analysis based on the FBM assumes that during its lifetime, an excited pyrene label covalently attached onto a polymer probes a sub-volume of the polymer coil which is referred to as a *blob*. The polymer coil is then divided into a cluster of *blobs* where the pyrene groups distribute themselves randomly according to a Poisson distribution. FBM analysis of the fluorescence decays yields N_{blob}, the number of monomers encompassed inside a *blob*, and k_{blob}, the rate constant of excimer formation between an excited and a ground-state pyrene both located inside a same *blob*. Of particular interest to this project, the product $<k_{blob} \times N_{blob}>$ has been reported to be a universal parameter that provides a quantitative measure of the internal chain dynamics of a polymer in solution in a manner similar to what T_g accomplishes for polymers in the bulk.[28]

In the present study, the FBM analysis was applied to the fluorescence decays acquired with a series of Py-Amylose constructs and poly(methyl acrylate)s randomly labeled with pyrene (Py-PMA) in DMSO. The chemical structure of Py-Amylose and Py-

PMA is provided in Table 1. PMA being a well-known flexible polymer with a T_g equal to 12 ^{o}C provided a valuable reference against which the internal dynamics of amylose in DMSO could be compared. The similar $<k_{blob} \times N_{blob}>$ values retrieved for the flexible PMA and rigid amylose in DMSO reflected a highly efficient excimer formation for the Py-Amylose constructs. This unexpectedly efficient excimer formation could only be possible if amylose formed a compact structure in DMSO to reduce the average distance between pyrenyl moieties. FBM analysis of the fluorescence decays of Py-Amylose in DMSO yielded an N_{blob} value of 11 ± 2 which was in excellent agreement with the maximum number of anhydroglucose units determined via molecular mechanics optimization that were required to enable excimer formation between two pyrene labels covalently attached to a helical amylose construct. To the best of our knowledge, this study represents the first attempt in the literature where the internal dynamics of amylose in DMSO were characterized by applying pyrene excimer fluorescence and use the results of this study to draw conclusions about the conformation of amylose in DMSO.

EXPERIMENTAL SECTION

Materials: Chemicals were purchased from Sigma-Aldrich (Milwaukee, WI) and used as received unless otherwise stated.

Characterization of amylose by intrinsic viscosity: The amylose sample used in these experiments had an intrinsic viscosity of 37 mL/g in DMSO at 25 ^{o}C corresponding to a weight-average molecular weight of 65,000 g.mol^{-1} based on a reported calibration curve.[10] However, since the pyrene-labeling procedure involved several precipitation cycles to remove unattached pyrene labels, the amylose sample was precipitated as many times as for the Py-Amylose samples. The intrinsic viscosity increased from 37 mL/g for the non-

precipitated sample to 43.7 (± 0.3) mL/g for the precipitated sample as shorter molecular weight chains were lost during the precipitations. Accordingly, a larger M_w value of 82,000 g.mol^{-1} for the precipitated amylose sample was found. Similar intrinsic viscosity values of 45.3 (±0.6) and 47,2 (±0.6) mL/g were obtained for the Py-Amylose samples labeled with 5.5 and 10 mol% pyrene, respectively. The similar intrinsic viscosity values obtained for the unlabeled and pyrene-labeled amylose samples suggest that the Py-Amylose samples have an M_w value around 80,000 g.mol^{-1}. Such an M_w value corresponds to a degree of polymerization of about 500 anhydroglucose units, considerably larger than the size of a *blob* determined by the FBM to equal 11 ± 2 units which ensures the validity of the FBM analysis for these Py-Amylose samples.

Synthesis of pyrene-labeled PMA (Py-PMA): The synthesis, purification, and characterization of the pyrene-labeled PMA samples has been described elsewhere.[28]

Synthesis of pyrene-labeled amylose (Py-Amylose): All Py-Amylose constructs were prepared in a similar manner. The synthesis of Py-Amylose with 7 mol% pyrene is described in more details hereafter. Amylose (0.5 g, 3 mmol in terms of anhydroglucose units) was dissolved in 20 mL of a 3:1 DMSO:DMF mixture at 60 °C until the solution was clear. DMF was added to DMSO to prevent the reaction mixture from freezing at 0 °C and since DMF is a poor solvent for amylose, the amount of DMF added was low enough to ensure that amylose was fully dissolved in this solvent mixture. Since the labeling reaction was inefficient, an 8-fold excess of the required amount of 1-pyrenebutyric acid (PBA) (0.5 g, 1.7 mmol) and a two-fold excess of 4-dimethylaminopyridine (DMAP, 0.05 g, 0.4 mmol) were dissolved in the DMSO/DMF mixture. The reaction mixture was then cooled in an ice bath followed by the addition of *N,N'*-diisopropylcarbodiimide (DIC) (0.4 mL, 2.7

mmol) dropwise under a nitrogen atmosphere. The reaction mixture was kept at 0 °C for 5 min and then left stirring in the dark for 48 hours at room temperature under nitrogen. The molar amount of amylose was kept constant for all reactions. The amounts of PBA, DMAP, and DIC could be adjusted to obtain the desired pyrene content. The Py-Amylose product was precipitated in cold methanol. The recovered product was redissolved in DMSO and reprecipitated in methanol. The precipitation cycle was repeated 3-5 times to remove any unreacted PBA. The final product was dried in a vacuum oven at room temperature overnight.

Table 1. Chemical structures of the pyrene-labeled polymers. Left: poly(methyl methacrylate), right: amylose.

Py-PMA	Py-Amylose
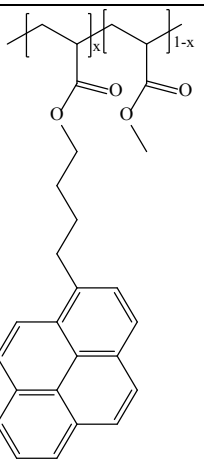	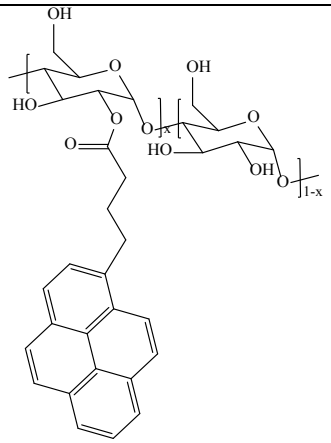

Pyrene content determination: The pyrene content, λ_{Py} expressed in mole of pyrene per gram of polymer, was determined using Equation 1. A mass, *m*, of dried Py-Amylose was carefully weighed before being dissolved in a known volume, *V*, of DMSO. The pyrene concentration [*Py*] was determined by UV-Vis absorption measurements applying Beer-

Lambert's Law to the pyrene absorption at 346 nm with an extinction coefficient of 41,400 $M^{-1}.cm^{-1}$ determined in the laboratory for PBA in DMSO. The molar fraction, x, of pyrene-labeled anhydroglucose units in Py-Amylose was determined by applying Equation 2 where M_{Glu} and M_{Py} represented the molar mass of the unlabeled and pyrene-labeled anhydroglucose unit equal to 162 and 432 $g.mol^{-1}$, respectively. A similar procedure was applied to determine the pyrene content of the Py-PMA samples which has been reported in an earlier publication.[28]

$$\lambda_{Py} = \frac{[Py]}{m/V} \tag{1}$$

$$x = \frac{M_{Glu}}{M_{Glu} - M_{Py} + 1/\lambda_{Py}} \tag{2}$$

Steady-State Fluorescence Measurements: Steady-state fluorescence spectra were acquired on a Photon Technology International LS-100 steady-state fluorometer with an Ushio UXL-75 Xenon lamp and a PTI 814 photomultiplier detection system. The spectra were obtained using the usual right angle geometry with a 346 nm excitation wavelength. The samples were dissolved in DMSO with pyrene concentration below 2×10^{-6} M to avoid intermolecular excimer formation. The fluorescence spectra were acquired with aerated and degassed solutions of Py-Amylose and Py-PMA. The solutions of the pyrene-labeled polymers in DMSO were degassed for 40 minutes by bubbling a gentle flow of nitrogen to remove oxygen, an efficient quencher of pyrene. The polymer solutions were degassed to investigate how strongly the pyrene monomer lifetime affected excimer formation. The monomer (I_M) and excimer (I_E) fluorescence intensities were obtained by integrating the

fluorescence spectra over the wavelength range of 373 – 379 nm and 500 – 530 nm, respectively.

Time-resolved fluorescence measurements: The monomer and excimer fluorescence decays were acquired with an IBH Ltd. time-resolved fluorometer using an IBH 340 nm NanoLED as the excitation source. Samples were prepared in the same manner as for the steady-state fluorescence experiments. Samples were excited at a wavelength of 346 nm and the monomer and excimer emission were collected at 375 nm and 510 nm, respectively. A cut off filter at 370 nm for the monomer and 500 nm for the excimer were used to reduce contamination of the fluorescence signal by light scattering. The fluorescence decays were acquired over 1024 channels using a time-per-channel of 1.02 or 2.04 ns/ch with 20,000 counts at the maximum for the instrument response function and decay curves.

Analysis of the fluorescence decays using the FBM: As described earlier, the FBM is a conceptual tool used to divide the macromolecular object (random coil, helix, polymeric aggregates, …) under study into a cluster of *blobs* where the pyrene labels covalently and randomly attached onto the macromolecule distribute themselves among the *blobs* according to a Poisson distribution.[29,30] The five pyrene species Py_{diff}*, Py_{k2}*, Py_{free}*, *E0**, and *ES** were considered within the FBM framework. The pyrene population Py_{diff}* represents the structural units of the polymer bearing a pyrene label diffusing slowly inside the polymer coil[28] or around the envelop of a polymeric helix.[27,31] These diffusive motions are described by the three FBM parameters which are $<n>$, the average number of ground-state pyrenes per *blob*, k_{blob}, the rate constant of excimer formation inside a *blob* which contains one excited pyrene and a single ground-state pyrene, and the product $k_e \times [blob]$ where k_e represents the exchange rate constant of the ground-state pyrenes between *blobs*

and [*blob*] is the local *blob* concentration inside the polymer coil. The second pyrene species, Py_{k2}*, represents those Py_{diff}* pyrene labels that have been brought in close proximity with a nearby ground-state pyrene through Brownian motions of the backbone and of the linker connecting the pyrene label to the macromolecule. An excimer *E*0* is then formed through a rapid rearrangement of the pyrene labels with a rate constant k_2 that is usually one order of magnitude larger than k_{blob}. The excimer can then emit fluorescence with a lifetime τ_{E0}. The random labeling of the polymer results in a small population of pyrenes that are isolated from each other along the backbone and cannot form excimer. This pyrene species emits as free pyrene in solution with the natural lifetime τ_M of the pyrene monomer and is referred to as Py_{free}*. After labeling, a short-lived pyrene species, *ES*, was observed in the excimer decays of Py-Amylose only and it emitted with a short lifetime τ_{ES} of 3.5 ns which was fixed in the analysis. The *ES** species is usually observed in pyrene-labeled macromolecules that form little excimer[32] such as the rigid Py-Amylose constructs. Equations S1 and S2 in SI have been shown to fit satisfyingly the fluorescence decays of the pyrene monomer and excimer for a number of polymers randomly labeled with pyrene.[24,26,27]

The fluorescence decays of the pyrene monomer and excimer were fitted globally with Equations S1 and S2, respectively. The parameters used in these equations were optimized with the Marquardt-Levenberg algorithm.[33] The unquenched lifetime of the pyrene monomer, τ_M, was determined from the monomer decay of a polymer sparingly labeled with pyrene where more than 80% of the total pre-exponential weight could be attributed to those isolated pyrene monomers that do not form excimer and emit with a lifetime τ_M. τ_M was found to equal 86 ns and 136 ns for Py-PMA and 89.5 ns and 135 ns

for Py-Amylose before and after degassing, respectively. The fit yielded the parameters $<n>$, k_{blob}, and $k_e[blob]$. The monomer decay analysis yielded the molar fractions f_{Mdiff}, f_{Mk2}, and f_{Mfree} which represent the contributions of the pyrene species Py_{diff}*, Py_{k2}*, and Py_{free}* to the monomer decays, respectively. In a similar manner, the excimer decay analysis with Equation 4 yielded f_{Ediff}, f_{Ek2}, f_{EE0}, and f_{EES} which represent the molar fractions of the pyrene species Py_{diff}*, Py_{k2}*, $E0$*, and ES* that contribute to the excimer decays, respectively. The fractions f_{Mdiff}, f_{Mk2}, f_{Mfree}, f_{Ediff}, f_{Ek2}, and f_{EE0} were then combined to determine the overall molar fractions f_{diff}, f_{k2}, f_{free}, and f_{E0} of the pyrene species present in solution. The mathematical expressions used for the molar fractions representing the different pyrene species have been provided in SI. The molar fraction f_{Mfree} together with $<n>$ and the pyrene content λ_{Py} defined in Equation 1 could be used to determine N_{blob}, the average number of structural units per *blob* whose expression is given in Equation 3.

$$N_{blob} = \frac{1 - f_{M_{free}}}{\lambda_{Py}} \frac{< n >}{[M_{Py}(x) + M_{Glu}(1-x)]} \tag{3}$$

The fits of the monomer and excimer fluorescence decays were considered good if the χ^2 was smaller than 1.2 and the residuals and the autocorrelation function of the residuals were randomly distributed around zero. A sample of the fit of the pyrene monomer and excimer fluorescence decays is given in Figure S2 in SI. The parameters retrieved from the FBM analysis of the decays are listed in Tables S1 – S3.

RESULTS AND DISCUSSION

Steady-state fluorescence spectra were acquired for degassed and undegassed Py-PMA and Py-Amylose solutions in DMSO and they are shown in Figures 1A and 1B. The intensity was normalized at 376 nm which corresponds to the 0-0 transition of pyrene in DMSO and set to an arbitrary value of 100. Figures 1A and 1B indicate that more pyrene excimer with its broad structureless emission at 480 nm was formed with increasing pyrene content due to the increased probability of encounter between the two pyrene labels. But before discussing the results obtained by steady-state fluorescence in more details, a number of control experiments needed to be carried out.

Since the purpose of this study was to investigate whether amylose adopts a helical conformation in DMSO, it was important to confirm that the excimer formation of Py-Amylose only occurred intramolecularly in DMSO. A helical conformation reflecting stronger polymer-polymer interactions could result in intermolecular interactions leading to intermolecular pyrene excimer formation. To ensure that this was not the case, Py-Amylose constructs with a low, intermediate, and high pyrene content of, respectively, 5.1, 7.5, and 14.9 mol% were dissolved in DMSO and the final concentration of these Py-Amylose solutions was adjusted to 3, 6, and 9 mg/L. Steady-state fluorescence spectra of the solutions were then acquired. The I_E/I_M ratio was determined and plotted as a function of Py-Amylose concentration in Figure 2. Within experimental error, the I_E/I_M ratio remained constant for the range of massic polymer concentrations used in this study. This result demonstrated that at these polymer concentrations, pyrene excimer formation only occurred intramolecularly for Py-Amylose in DMSO.

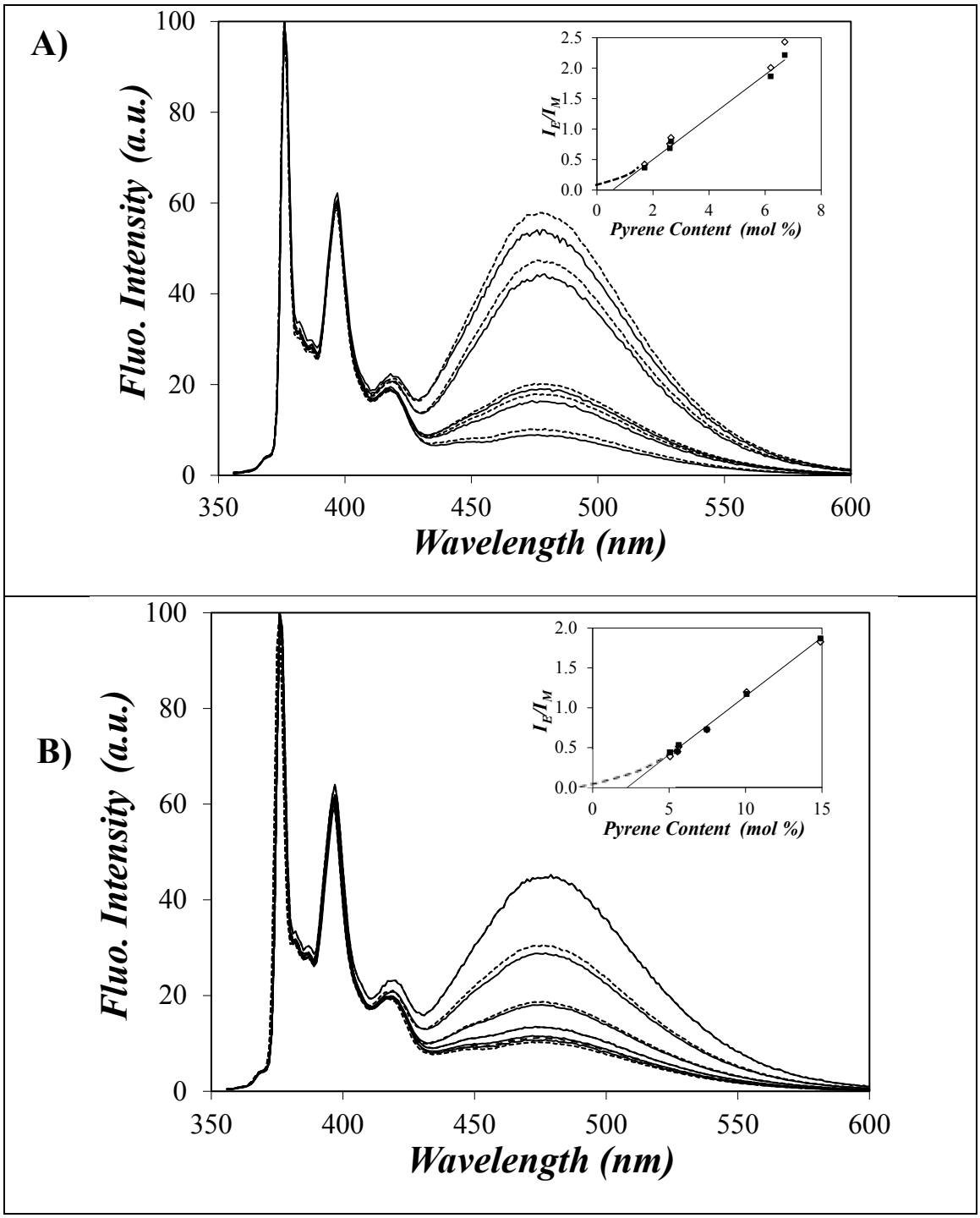

Figure 1. Steady-state fluorescence spectra of degassed (·····) and undegassed (———) A) Py-PMA in DMSO and B) Py-Amylose in DMSO. Insets: Plots of I_E/I_M ratios as a function of pyrene content for A) Py-PMA and B) Py-Amylose (■) before degassing and (□) after degassing. [Py] = 2.5×10^{-6} M, λ_{ex} = 346 nm.

When studying pyrene-labeled polymers, the I_E/I_M ratios are typically used as a qualitative measure of the pseudo-unimolecular rate constant of excimer formation that includes the local pyrene concentration sensed by an excited pyrene.[34] The I_E/I_M ratios of Py-PMA and Py-Amylose were found to increase with pyrene content in the insets of Figure 1 reflecting the faster kinetics of pyrene excimer formation resulting from an increased local pyrene concentration. It was noticeable however that none of the lines representing the I_E/I_M ratios passed through the origin. This behavior is a result of excimer formation being a local phenomenon that occurs between an excited and a ground-state pyrene label that are separated by a few tens of monomers, as will be found later using the FBM analysis. Consequently, a sufficiently high number of pyrene labels need to be covalently attached to the polymer to bring the pyrene labels within striking range from each other to form an excimer. According to the inset of Figure 1, no pyrene excimer could be formed until a threshold pyrene content of ~ 0.6 mol% for Py-PMA and ~ 2.2 mol% for Py-Amylose was reached.

The slope ($m(I_E/I_M)$) of the straight lines drawn in the insets of Figure 1 reflected the efficiency of pyrene excimer formation and it was found to equal 0.35 for Py-PMA which is significantly larger than that of 0.15 found for Py-Amylose. At first glance, this result suggests that excimer formation is less efficient for Py-Amylose as would be expected from its backbone rigidity. However this conclusion is somewhat misleading because each anhydroglucose unit contributes 5 backbone atoms to the chain contour length of Py-Amylose compared to 2 backbone atoms contributed by each methyl acrylate monomer to the chain contour length of Py-PMA. In fact, on a "per backbone atom" basis,

$m(I_E/I_M)$ of Py-Amylose would be 5 times larger yielding an $m(I_E/I_M)$ value of 0.75 comparable to the value of 0.70 obtained by multiplying $m(I_E/I_M)$ for Py-PMA by 2.

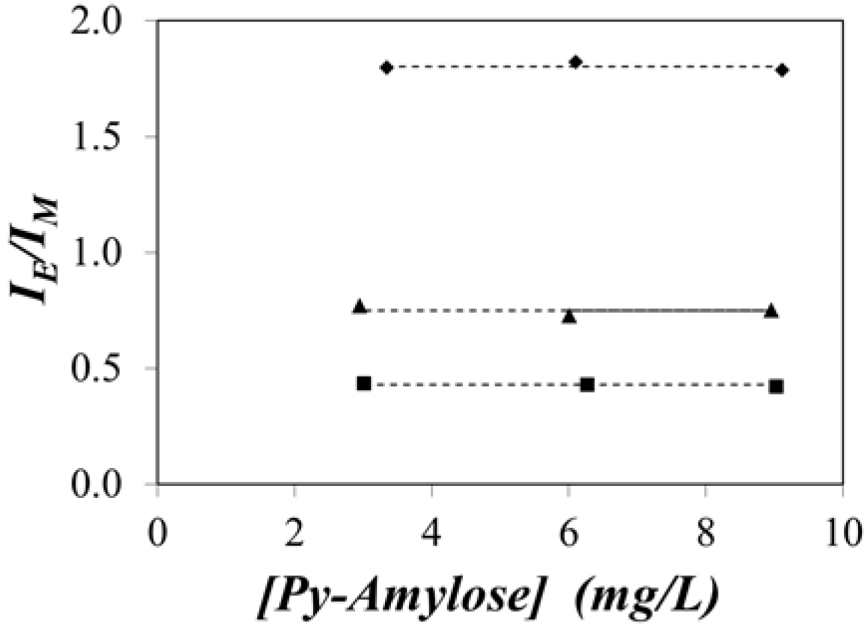

Figure 2. Plot of I_E/I_M as a function of Py-Amylose concentration in DMSO. (■) 5.05 mol%, (▲) 7.5 mol% and (◆) 14.9 mol%.

It is important to note at this point that the I_E/I_M ratio obtained from the analysis of the steady-state fluorescence spectra is a parameter that represents all pyrene species that contribute to the monomer and excimer fluorescence. These include the species Py_{free}* that does not form excimer and $E0$* that forms excimer instantaneously upon direct excitation. Consequently, Py_{free}* and $E0$* do not provide any information on the dynamic process of excimer formation. In fact, beside the contribution of Py_{diff}*, all other pyrene species contributing to the fluorescence signal can be viewed as fluorescent impurities that contaminate the dynamic information pertaining to excimer formation in the pyrene-labeled macromolecule. To differentiate between the contributions of the different pyrene

species and most importantly to isolate the contribution from Py_{diff}* reporting on the internal dynamics of the pyrene-labeled macromolecule, analysis of the time-resolved fluorescence decays needs to be conducted.

Global FBM analysis of the monomer and excimer decays using Equations S1 and S2 was conducted first by letting all parameters beside the lifetimes of the monomer (τ_M) and the short-lived excimer (τ_{ES}) float. The rate constant k_2 obtained for a given polymer series was then averaged and its averaged value was fixed in the decay analysis which was then repeated. This procedure has been found to yield a much tighter set of values for the parameters $<n>$, k_{blob}, and $k_e[blob]$ which represent the internal dynamics of the macromolecules under investigation.[28,35] All parameters retrieved from the FBM analysis of the decays are listed in Tables S1-3.

The fits were good (see Figure S2). Within experimental error, the excimer lifetime (τ_{E0}) remained constant with pyrene content and equal to 41 (±2) ns and 49 (±2) ns for aerated and degassed Py-PMA samples and 48 (±3) ns and 56 (±3) ns for aerated and degassed Py-Amylose, respectively. These τ_{E0} values are reasonable for pyrene excimer in an organic solvent.[36] Larger τ_{E0} values were obtained after degassing as expected. Interestingly, the τ_{E0} values were also larger for Py-Amylose than for Py-PMA suggesting that Py-Amylose provides a more rigid environment which resulted in a longer excimer lifetime. Excimer formation in a *blob* that contained one excited pyrene and one ground-state pyrene occurred with a rate constant k_{blob} equal to 1.6 (±0.2)×10^7 s^{-1} and 1.8 (±0.2)×10^7 s^{-1} for degassed and aerated Py-Amylose solutions and 1.1 (±0.1)×10^7 s^{-1} and 1.2 (±0.1)×10^7 s^{-1} for degassed and aerated Py-PMA solutions, respectively. The rate constant k_2 describing the rapid rearrangement of the pyrene labels before forming an

excimer was fixed to 1.4 and 1.7×10^8 s^{-1} for aerated and degassed Py-PMA solutions and 2.0×10^8 s^{-1} for both aerated and degassed Py-Amylose solutions. The k_2 values were thus one order of magnitude larger than k_{blob} reflecting the rapid rearrangement of the pyrene species to form an excimer. The values of $<n>$ and f_{Mfree} obtained from the decay analysis were then introduced in Equation 5 to calculate N_{blob} which was plotted as a function of pyrene content in Figure 3A. Within experimental error, N_{blob} was found to remain constant with pyrene content and increasing the monomer lifetime from 89.5 ns to 135 ns for Py-Amylose by degassing the solution did not lead to a substantially larger blob size. The N_{blob} value averaged over all pyrene contents, $<N_{blob}>$, was found to equal 10 ± 1 anhydroglucose units for amylose before degassing and 11 ± 2 anhydroglucose units after degassing resulting in an overall average $<N_{blob}>$ value of 11 ± 2. On the other hand, $<N_{blob}>$ was found to equal 43 ± 2 monomer units for PMA before degassing and 46 ± 4 units after degassing resulting in an overall $<N_{blob}>$ value of 45 ± 4 units. A previous study of Py-PMA in tetrahydrofuran (THF) reported an $<N_{blob}>$ value of 59 ± 5.[28] The smaller blob size obtained in DMSO can be rationalized by the viscosity difference between THF (η = 0.47 mPa.s at 25 °C) and DMSO (η = 1.99 mPa.s at 25 °C). The higher viscosity of DMSO reduced the mobility of the pyrene labels of Py-PMA resulting in a smaller volume being probed by pyrene during its lifetime.

When plotted against pyrene content in Figure 3B, $k_{blob}\times N_{blob}$ was also found to remain constant with pyrene content. The value of the product $k_{blob}\times N_{blob}$ for amylose averaged over all pyrene contents, namely $<k_{blob}\times N_{blob}>$, was found to equal 1.7 $(\pm0.1)\times10^8$ s^{-1} before and after degassing, respectively. By comparison, $<k_{blob}\times N_{blob}>$ was found to equal 5.2 $(\pm0.5)\times10^8$ s^{-1} and 4.8 $(\pm0.5)\times10^8$ s^{-1} for PMA before and after

degassing, respectively. However, direct comparison of the $<N_{blob}>$ and $<k_{blob}\times N_{blob}>$ values between amylose and PMA is biased since both parameters are calculated in terms of the number of monomers constituting a *blob* which contribute differently, in terms of backbone atoms, to the chain contour length of the polymers. This difference can be corrected by reporting $<N_{blob}>$ and $<k_{blob}\times N_{blob}>$ in terms of backbone atoms instead of monomer units. With only two chain atoms per monomer, PMA would have $<N_{blob}>$ and $<k_{blob}\times N_{blob}>$ values equal to 90 (± 4) and 1.0 (± 0.1)$\times 10^9$ s^{-1} in terms of chain atoms, respectively. Similarly, amylose with its five chain atoms per anhydroglucose unit contributing to the contour length of the polymer would have $<N_{blob}>$ and $<k_{blob}\times N_{blob}>$ values of 55 (± 10) and 0.85 (± 0.05)$\times 10^9$ s^{-1} in terms of chain atoms, respectively. Interestingly, the product $<k_{blob}\times N_{blob}>$ in terms of chain atoms of amylose and PMA becomes comparable for flexible PMA and rigid amylose after this correction. Since $<k_{blob}\times N_{blob}>$ is a measure of the efficiency of excimer formation, that similar $<k_{blob}\times N_{blob}>$ values were obtained for Py-PMA and Py-Amylose suggests that both macromolecular constructs form excimer with a similar efficiency.

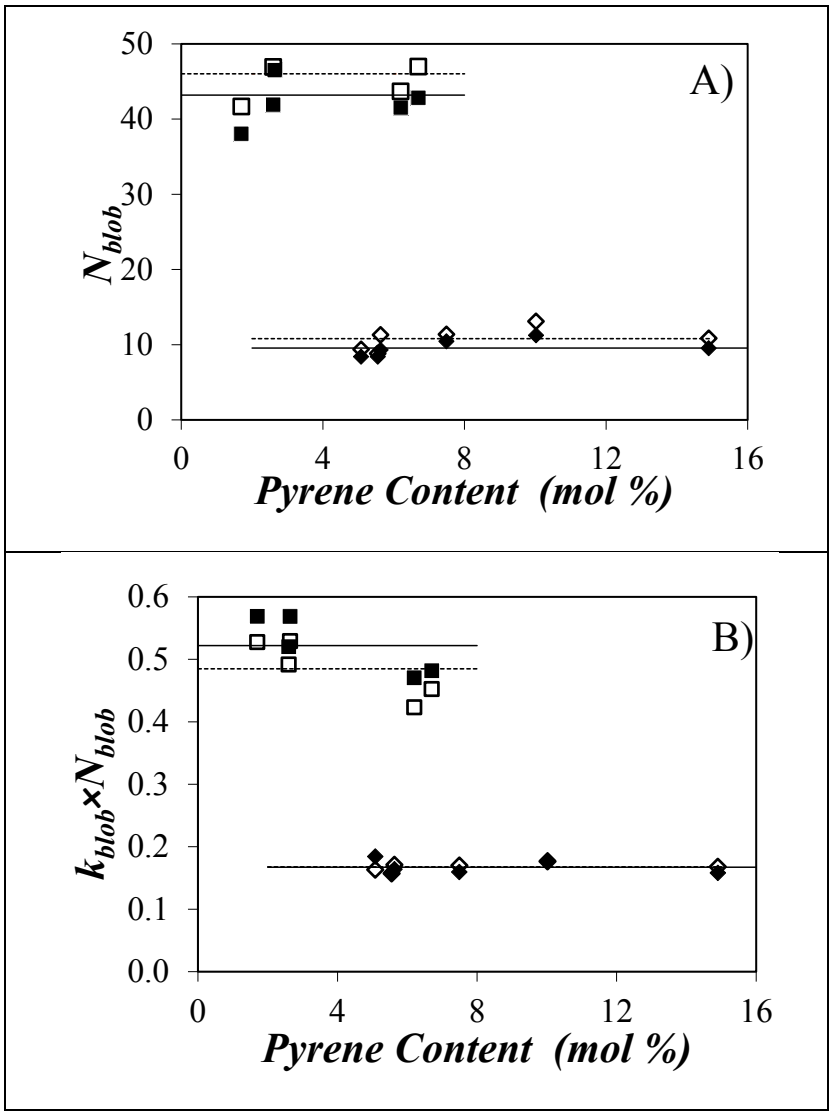

Figure 3. Plot of A) N_{blob} and B) $k_{blob} \times N_{blob}$ as a function of pyrene content. (□) PMA before degassing, (■) PMA after degassing, (◇) amylose before degassing, and (◆) amylose after degassing.

For polymers having a similar conformation, such as poly(alkyl methacrylate)s with different side chain lengths adopting a random coil conformation in tetrahydrofuran, the product $<k_{blob} \times N_{blob}>$ faithfully reflects the chain mobility of different polymer backbones in solution.[28] However the amylose backbone is certainly more rigid compared

to that of PMA. Thus the unexpectedly large value of $<k_{blob} \times N_{blob}>$ cannot be explained by the higher mobility of the amylose backbone. Another factor that can increase the rate constant of excimer formation is the local pyrene concentration. For a similar level of labeling, a more compact conformation of the polymer backbone would bring the pyrene groups closer to each other leading to a higher local pyrene concentration which would increase the rate of pyrene excimer formation. A random coil conformation of amylose would be unlikely to provide this level of compactness. In turn, this unexpectedly large $<k_{blob} \times N_{blob}>$ value could be a result of amylose adopting a helical conformation in DMSO.

In fact, the finding in an earlier report that pyrene excimer formation occurred as efficiently for a rigid polycarbonate (PC) as for a much more flexible poly(dimethyl siloxane) both end-labeled with pyrene led to the conclusion that the more rigid PC backbone was adopting a helical conformation in solution.[37] In addition, even though $<N_{blob}>$ for amylose is smaller than for PMA, a *blob* consisting of 11 anhydroglucose monomers represents a large volume to probe for a pyrene pendant attached to the backbone via a short butyl linker. In this context, a study of the physical dimensions of the space probed by an excited pyrene bound to amylose adopting an extended random coil or a compact helical conformation would be quite informative to assess which conformation of amylose in DMSO is best represented by the $<N_{blob}>$ values obtained by fluorescence.

To this end, the *HyperChem* software (version 7.04) was used to create amylose constructs having a helical and random coil conformation. Even though the crystal structure of amylose has been well characterized by X-ray, no structural information could be found in the literature regarding a helical conformation of amylose in DMSO. Therefore, two possible helical structures were considered in this study to test the effect of geometry on

the *blob* size. The first helix was optimized from the default conformation calculated by *HyperChem* for an amylose construct made of 40 anhydroglucose units. The optimized structure was a symmetrical 9 fold helix which is shown in Figure 4A. The number of anhydroglucose units per turn in the helix is slightly larger than the reported literature values obtained from the analysis of the crystal structure of amylose. For comparison purpose, a second helical structure for amylose was imported into *HyperChem* based on the X-ray results reported by Nishiyama et al.[38] The optimized structure is a 7 fold helix which is shown in Figure 4B. In order to obtain an amylose construct that would be more representative of a random coil conformation, the *HyperChem* software was employed to build an amylose chain made of 20 anhydroglucose units. It was then extended to a distance that was longer than its contour length and allowed to relax into the conformation shown in Figure 5.

FBM analysis of the decays found that an amylose *blob* was made of 11 ± 2 anhydroglucose units. Based on the FBM framework, this result implies that two pyrenes can overlap and form an excimer when they are located within a section of the helix made of 11 units. The symmetry of the helix imposes that if a pyrene moiety is located at the center of the *blob*, an excimer will be formed if a second pyrene is located within 5 residues on either side of the first pyrene. To investigate whether this was the case for the constructs shown in Figures 4 and 5, the following procedure was applied. A first structure was created where one pyrene butyric acid pendant was attached onto the 3rd residue along the helix and a second pyrene butyric acid was attached onto the 4th residue. The numbering of the carbon atoms used to represent the anhydroglucose unit or pyrene can be viewed in Figure S1 in SI. For both helical conformations, the C6 hydroxyl group of the

anhydroglucose unit was found to be closer to the central cavity of the helix which led to poor accessibility. Therefore the pyrene labels were attached to the C2 instead of the C6 hydroxyl group of the polysaccharide since the latter hydroxyl appeared to be less accessible.

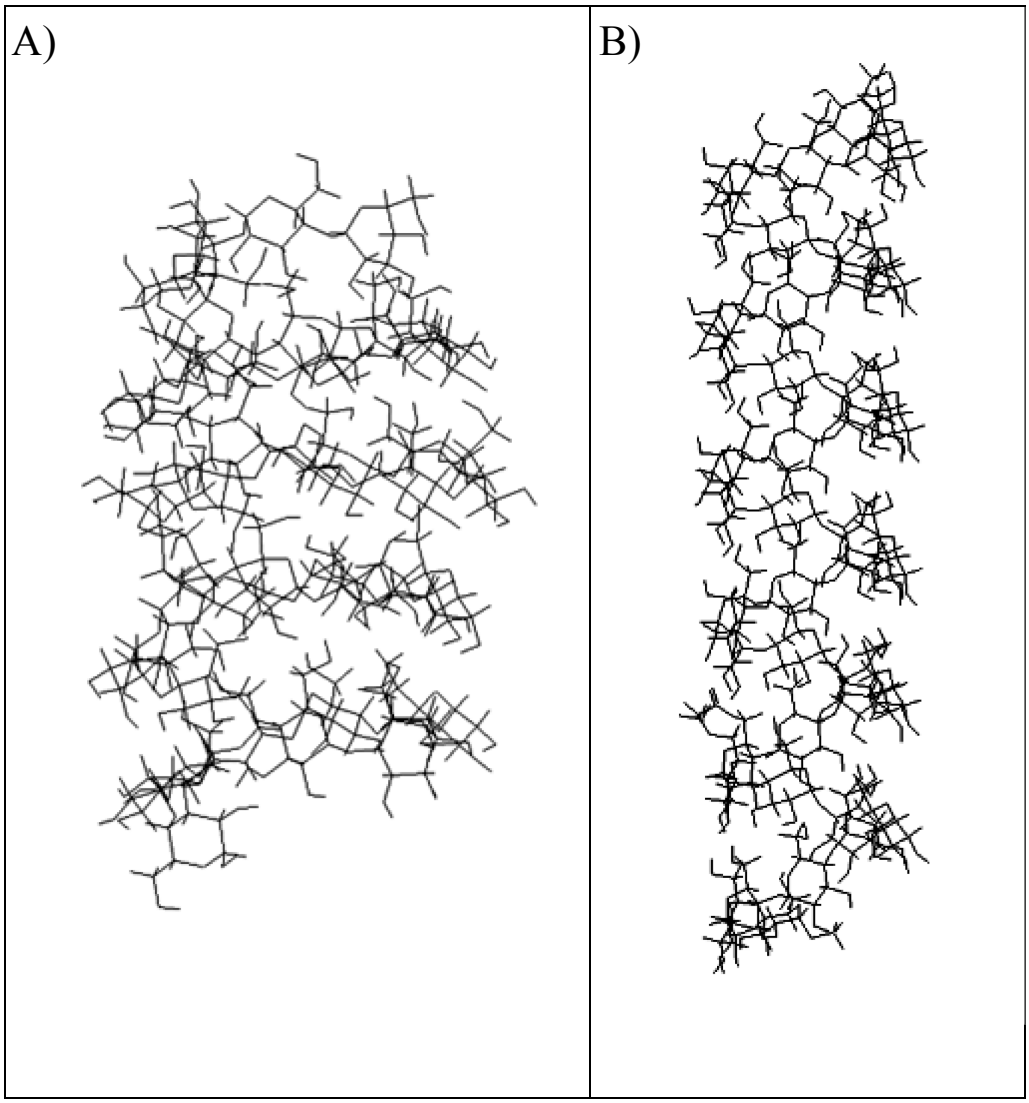

Figure 4. Two possible helical structures for amylose: A) 9-fold and B) 7-fold helix.

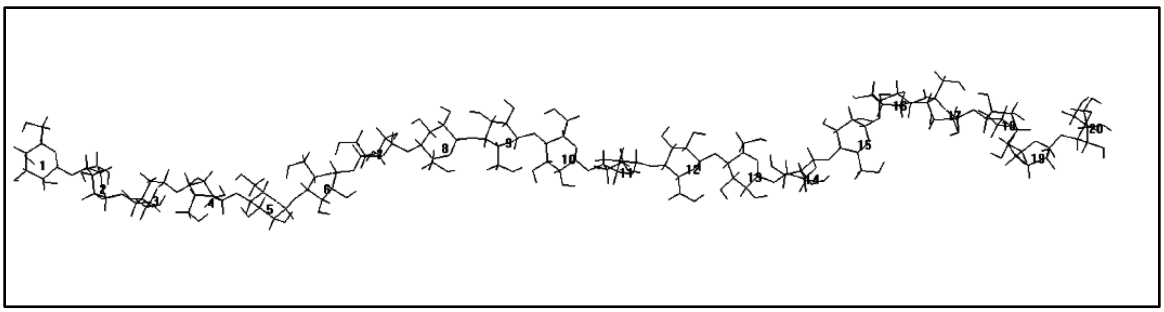

Figure 5. Relaxed random coil conformation of amylose.

A molecular mechanics optimization using the Fletcher-Reeves algorithm was performed during which the following constraints were imposed. The distance separating the carbons C2 or C7 of a pyrene label from the carbons C2 or C7 of the other pyrene label was set to equal 3.4 Å by the end of the molecular mechanics optimization.[27,31] Whether the C2 or C7 carbons were selected depended on which orientation of the pyrenes would result in the best overlap between the two pyrenes. None of the backbone atoms of the helices were included in the optimization so that the polysaccharide backbone was not altered during the optimization. Only pyrene and the atoms connecting pyrene to the anhydroglucose unit where allowed to be displaced during the optimization. At the end of the optimization, the extent of overlap between the two pyrenes was estimated by calculating the number of carbon atoms of the first pyrene molecule which were covered by the frame of the second pyrene molecule. This procedure was repeated by keeping the first pyrene on the 3rd residue and moving the second pyrene moiety from the 4th to the 33rd residue of the helix in one residue increments. An illustration of the extent of overlap is shown in Figure 6 using the 7-fold amylose helix. When attached on two adjacent anhydroglucose units, the two pyrene labels can be arranged in a conformation resulting in a good overlap involving 9 carbons. However, when separated by 21 anhydroglucose units,

the two pyrene pendants could not overlap even after full extension of the butyl linkers connecting the pyrene labels to the amylose backbone.

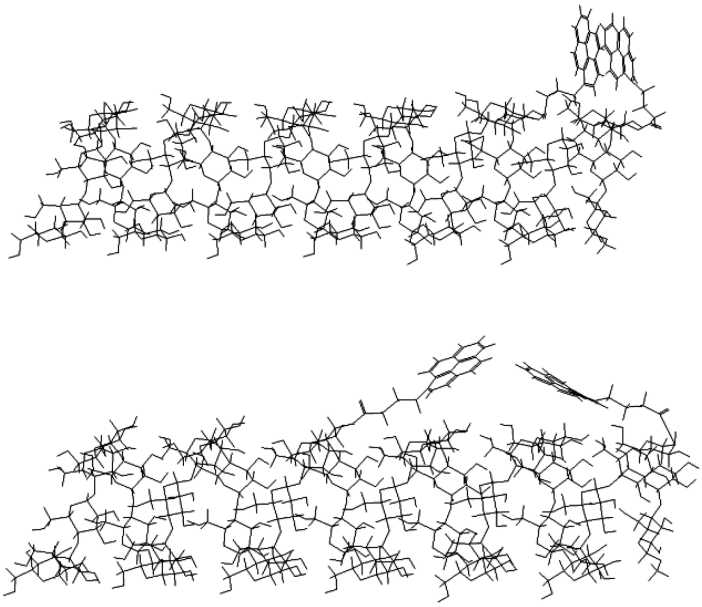

Figure 6. An illustration of the ability of two pyrene groups to overlap when separated by 7 anhydroglucose units (Top: good overlap) and 21 anhydroglucose units (Bottom: no overlap)

Geometry optimization of the pyrene labels attached to amylose adopting a random coil conformation was conducted in a similar manner except for the following two differences. First, since the three hydroxyl groups were fully accessible in the random coil conformation, the pyrene moiety was attached on the more reactive C6 hydroxyl which was now accessible for labeling and enabled the farthest reach for excimer formation. Second, it was also observed that the orientation of an individual anhydroglucose unit changed along the chain. Consequently a series of optimizations were carried out with one pyrene attached on the first anhydroglucose unit and moving the second pyrene from the 2^{nd} to the 8^{th} anhydroglucose unit in one anhydroglucose unit increments, and the extent of

overlap between the two pyrenes was recorded in each case. A second series of optimizations were then conducted with the first pyrene attached onto the 2nd anhydroglucose unit and displacing the second pyrene from residues 3 to 9 in one residue increments. The extent of overlap was recorded. In total, 8 sets of optimizations were carried out and the final results obtained to characterize the extent of overlap between two pyrene labels was averaged. For all simulations, a good overlap between two pyrenes was characterized by one pyrene having at least 7 carbon atoms covered by the area of the second pyrene as has been done earlier.[27,31]

The results obtained from the molecular mechanics optimizations based on two helix conformations, one with a 7-fold and the other with a 9-fold periodicity, are shown in Figure 7. The similar trends obtained for the 7-fold and 9-fold helices indicated that the extent of overlap depends strongly on the position of the pyrene pendants along the helix but little on whether the helices had a 7-fold or a 9-fold periodicity. The overlap was nonexistent when two pyrene moieties were three anhydroglucose units apart since they pointed to opposite directions away from the helix. The overlap was restored when the two pyrene moieties were located on two anhydroglucose units separated by one helical turn. The trends obtained by optimization of the 7-fold and 9-fold helices were quite similar. Both trends demonstrated that two pyrenes yielded a good overlap if the anhydroglucose units, onto which the pyrenes were attached, were separated by 1, 2, 7, 8, and 9 anhydroglucose units or 1, 2, 8, 9, and 10 anhydroglucose units for the 7-fold and 9-fold helices, respectively, both helices yielding a set of five residues enabling good overlay between two pyrene labels. Consequently, the results from the molecular mechanics optimization of the amylose helices suggested that a *blob* was made of 2×5+1 = 11

anhydroglucose units, in excellent agreement with the $<N_{blob}>$ value of 11 ± 2 obtained by FBM analysis of the Py-Amylose decays.

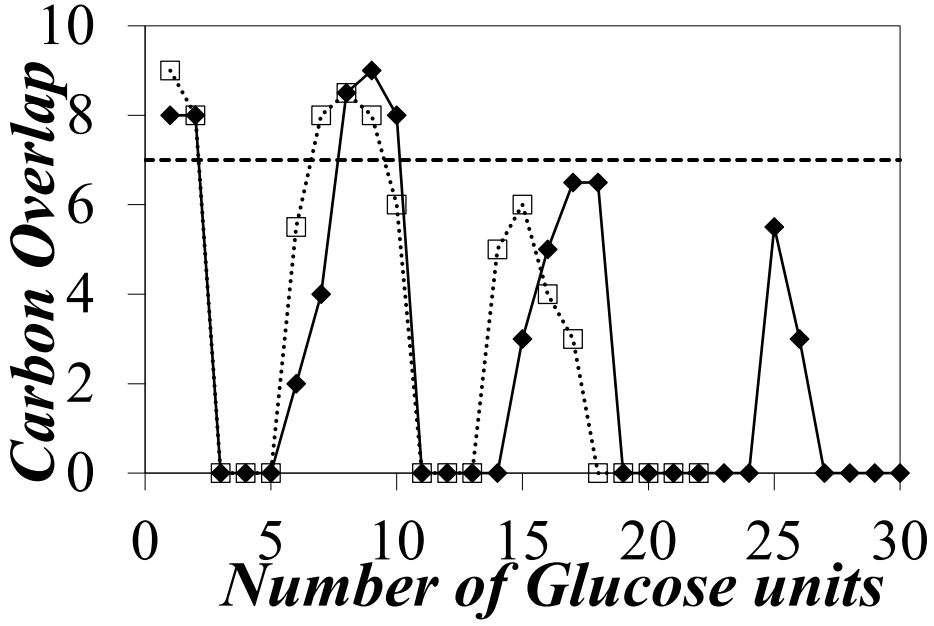

Figure 7. Pyrene carbon-overlap as a function of the number of anhydroglucose units between pyrene groups obtained via molecular mechanics optimization of an amylose helix. (□) 7 fold helix, (◆) 9 fold helix.

The results obtained by molecular mechanics optimization of an extended amylose conformation more representative of a random coil were plotted in Figure 8. The trends showed that the extent of overlap decreased rapidly with increasing separation distance if amylose formed a random coil in solution. Poor overlap was obtained when two pyrene pendants were more than four anhydroglucose units apart along the extended polysaccharide. A separation of 3 anhydroglucose units yielded a 50% chance of having a good overlap between two pyrene labels and a good overlap was always obtained if the pyrene labels were separated by 1 or 2 anhydroglucose units. These results led to the

conclusion that, if Py-amylose adopts a random coil conformation, the blob size must be less than 3×2+1=7 anhydroglucose units which is much smaller than the $<N_{blob}>$ value of 11 ± 2 obtained from the FBM analysis, and thus disfavors the possibility of amylose adopting an extended conformation in DMSO. Consequently, the results obtained by FBM analysis of the fluorescence decays and molecular mechanics optimization strongly suggest that the conformation of amylose in DMSO is that of a rigid helix.

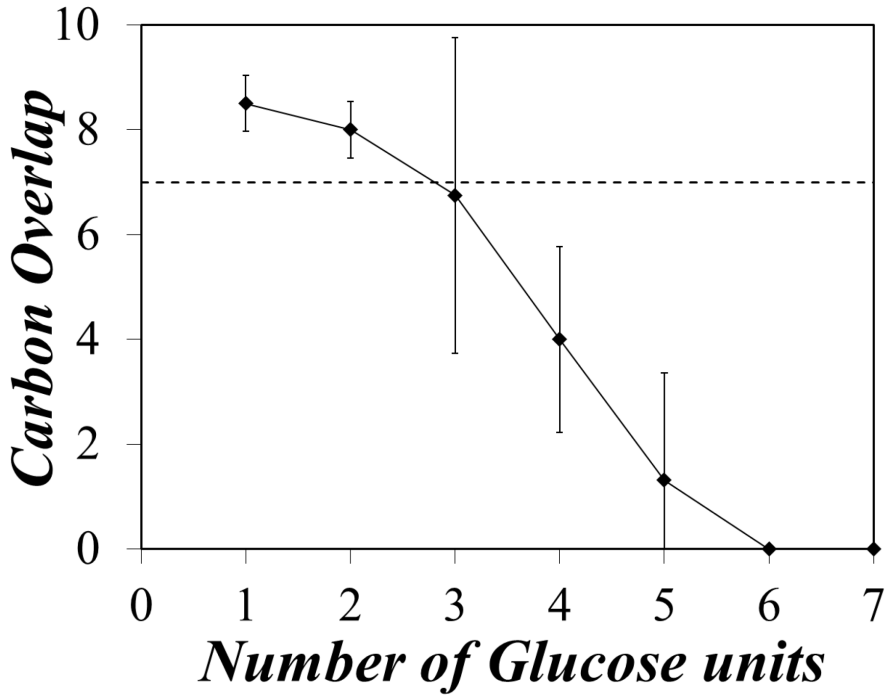

Figure 8. Pyrene carbon-overlap as a function of the number of anhydroglucose units between pyrene groups obtained via molecular mechanics optimization of an amylose random coil.

Further indication that amylose adopted a compact conformation in DMSO was obtained by plotting f_{E0} versus pyrene content for Py-PMA and Py-Amylose. The molar fraction f_{E0} represents the pyrene labels involved in pre-stacked pyrene dimers before excitation. Due to the random labeling of the polymers, higher pyrene contents led to a

smaller distance between the pyrene groups resulting in higher f_{E0} values. As shown in Figure 9, f_{E0} increased with pyrene content for both Py-PMA and Py-Amylose. Interestingly, f_{E0} for Py-Amylose was much higher than the value obtained for Py-PMA at a same pyrene content. This trend is unexpected considering that one anhydroglucose unit introduces 5/2 = 2.5 times more backbone atoms into the polymer than one methyl acrylate monomer. Consequently, the pyrene labels should be much more spread out along Py-Amylose for a same pyrene content compared to Py-PMA and thus generate much less pyrene aggregation. That this was not the case indicated that the pyrene pendants attached on the backbone of amylose were located in a compact environment which could only be explained by amylose forming a helical structure in DMSO. A similar enhancement in the f_{E0} values retrieved from the FBM analysis of the fluorescence decays acquired for a series of α–helical poly(*L*-glutamic acid)s randomly labeled with pyrene has been reported earlier.[31] It would appear that the enhanced pyrene aggregation observed for linear polymers adopting a helical conformation might be a general phenomenon resulting from the enhanced compactness of the structured macromolecules.

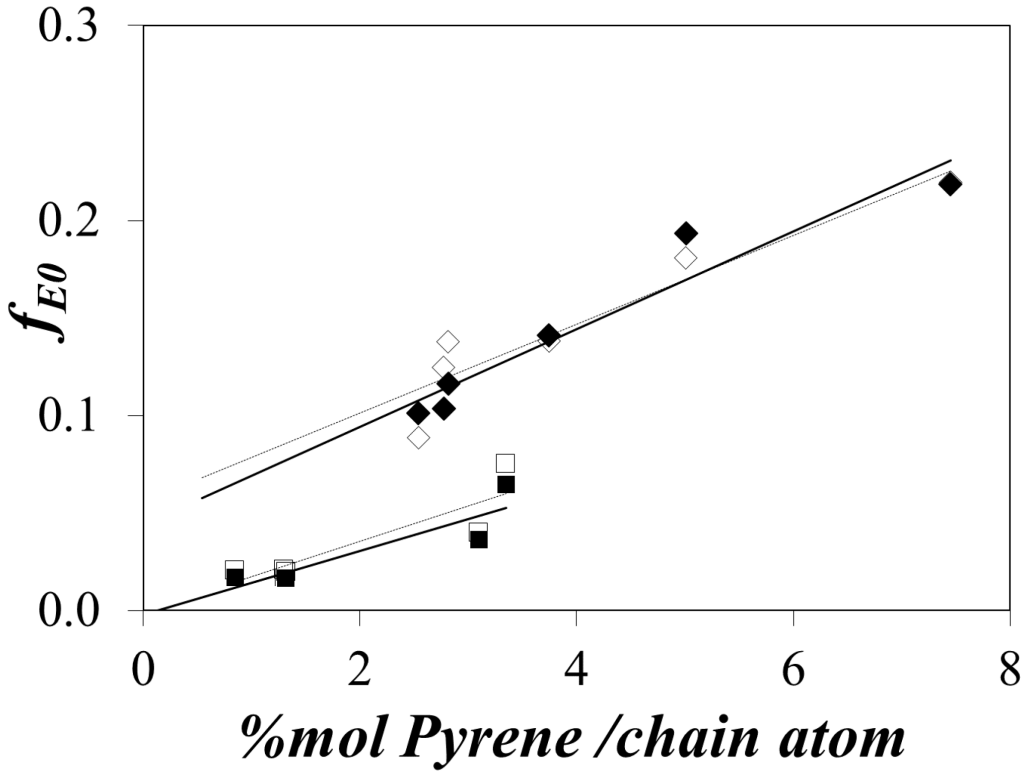

Figure 9. f_{EO} as a function of pyrene content/chain atom. (■) Py-PMA before degassing, (□) Py-PMA after degassing, (◆) Py-Amylose before degassing, (◇) Py-Amylose after degassing.

CONCLUSIONS

A series of Py-Amylose constructs were synthesized and their chain dynamics were characterized in DMSO by steady-state and time-resolved fluorescence. As a comparison, a flexible polymer, Py-PMA, was studied under the same conditions. Analysis of the steady-state fluorescence spectra to determine $m(I_E/I_M)$ based on the plots presented in Figure 1 showed that amylose formed excimer less efficiently compared to PMA if the pyrene content was expressed in mole of pyrene per mole of polymer structural unit. However, $m(I_E/I_M)$ became similar for Py-Amylose and Py-PMA if the pyrene content was

expressed in mole of pyrene per backbone atom indicating that both polymers formed excimer as effectively. Since the steady-state fluorescence spectra account for the contributions of all the pyrene species present in solution, quantitative information on the internal dynamics of the macromolecules was obtained by applying the FBM analysis to the fluorescence decays. One strength of the FBM analysis is that it differentiates between the different pyrene species that contribute to the monomer and excimer decays. The FBM analysis revealed that amylose had a significantly larger level of pyrene aggregation compared to the PMA samples with a similar labeling level. This result was a consequence of a more compact conformation adopted by amylose in DMSO compared to the more flexible PMA backbone. More importantly, FBM analysis yielded $<N_{blob}>$ and $<k_{blob} \times N_{blob}>$ values which reflected the polymer chain dynamics of the samples. Interestingly, $<k_{blob} \times N_{blob}>$ was comparable for amylose and PMA when expressed in terms of chain atoms. This unexpectedly large value of $<k_{blob} \times N_{blob}>$ for amylose could not be rationalized by an enhanced mobility of the more rigid amylose backbone. Rather this result indicated that the pyrene pendants attached onto the amylose backbone were probing a compact environment which was compatible with amylose adopting a helical conformation in DMSO.

To further confirm that this was indeed the case, molecular mechanics optimizations were conducted to examine how far two pyrene labels could encounter along an amylose backbone adopting different conformations. The optimization results obtained assuming that amylose adopted a random coil conformation yielded a blob size smaller than seven anhydroglucose units which disagreed with the N_{blob} value of 11 ± 2 anhydroglucose units obtained experimentally from the FBM analysis of the fluorescence

decays. In contrast, when amylose adopted a helical structure, the more compact geometry of amylose resulted in a blob size of eleven anhydroglucose units according to the molecular mechanics optimizations. This result was in excellent agreement with the results obtained by the FBM analysis. In view of the above, the fluorescence measurements conducted on the Py-Amylose constructs in combination with the molecular mechanics optimizations carried out with *HyperChem* demonstrated that amylose formed a rigid helix in DMSO. As it turns out, this study represents the second example where pyrene excimer fluorescence is applied to determine the helical conformation of a macromolecule in solution, the first example being for poly(*L*-glutamic acid).[27,31] It suggests that pyrene excimer fluorescence constitutes a robust analytical means to probe the compact conformation of condensed macromolecules by taking advantage of the restricted spatial range of pyrene encounters that lead to excimer formation upon contact.

ACKNOWLEDGMENTS

The authors thank NSERC and EcoSynthetix for generous financial support.

REFERENCES

1. Annable, T.; Buscall, R.; Ettelaie, R.; Whittlestone, D. The Rheology of Solutions of Associating Polymers: Comparison of Experimental Behavior with Transient Network Theory. *J. Rheol.* **1993**, *37*, 695-726.
2. Krejtschi, C.; Hauser, K. Stability and Folding Dynamics of Polyglutamic Acid. *Eur. Biophys. J.* **2011**, *40*, 673-685.

3. Costas, T.; Seixas de Melo, J. S. The Effect of g-Cylcodextrin Addition in the Self-Assembly Behavior of Pyrene Labeled Poly(acrylic acid) with Difference Chain Sizes. *J. Polym. Sci. A*: *Polym. Chem.* **2008**, *46*, 1402-1415.
4. Banks, W.; Greenwood, C. T. The Hydrodyhamic Behaviour of Native Amylose in Good Solvents. *Carbohydr. Res.* **1968**, *7*, 414-420.
5. Banks, W.; Greenwood, C. T. Amylose: A Non-Helical biopolymer in Aqueous Solution. *Polymers* **1971**, *12*, 141-145.
6. Banks, W.; Greenwood, C. T. The Conformation of Amylose in Alkaline Salt Solution. *Carbohydr. Polym.* **1972**, *21*, 229-234.
7. Everett, W.; Foster, J.F. The Conformation of Amylose in Solution *J. Am. Chem. Soc* **1959**, *81*, 3464-3469.
8. Cowie, J. M. G. Studies on Amylose and its Derivatives. Part I. Molecular Size and Configuration of Amylose Molecule in Various Solvents *Makromol. Chem.* **1961**, *42*, 230-247.
9. Fujii, M.; Honda, J.; Fujita, H. Dilute Solution of Amylose in Dimethyl Sulfoxide. *Biopolymers* **1973**, *12*, 1177-1195.
10. Nakanishi, Y.; Norisuye, T.; Teramoto, A. Conformation of Amylose in Dimethyl Sulfoxide. *Macromolecules* **1993**, *26*, 4220-4225.
11. Cheetham, N. W. H.; Tao, L. Amylose Conformational Transitions in Binary DMSO/Water Mixtures. *Carbohydr. Polym.* **1998**, *35*, 287-295.
12. St-Jacques, M.; Sundarajan, P.R.; Taylor, K.J.; Marchessault, R.H. Nuclear Magnetic Resonance and Conformational Studies on Amylose in Aqueous Solution *Biopolymers* **1976**, *12*, 65-78.

13. Ree, D. A. Conformational Analysis of Polysaccharides. V. Characterization of Linkage Confirmations (Chain Conformations) by Optical Rotation at a Single Wavelength. Evidence for Distortion of Cyclohexaamylose in Aqueous Solution. Optical Rotation and the Amylose Conformation. *J. Chem. Soc. (B)* **1970**, 877-884.
14. Tusch, M.; Krüger, J.; Fels, G. Structural Stability of V-Amylose Helices in Water-DMSO Mixtures Analyzed by Molecular Dynamics. *J. Chem. Theory Comput.* **2011**, *7*, 2919-2928.
15. Cuniberti, C.; Perico, A. Intramolecular Excimers and Micro-Brownian Motion of Flexible Polymer Molecules in Solution. *Eur. Polym. J.* **1977**, *13*, 369-374.
16. Martinho, J. M. G.; Winnik, M. A. Excluded Volume Effects on the End-to-End Cyclization of Polystyrene in Mixed Solvents. *Macromolecules* **1986**, *19*, 2281-2284.
17. Kanagalingam, S.; Ngan, C.F.; Duhamel, J. Effect of Solvent Quality on the Level of Association and Encounter Kinetics of Hydrophobic Pendants Covalently Attached onto a Water-Soluble polymer. *Macromolecules* **2002**, *35*, 8560-8570.
18. Zhang, M.; Duhamel, J. Effect of Solvent Quality toward the Association of Succinimide Pendants of a Modified Ethylene-Propylene Copolymer in Mixtures of Toluene and Hexane. *Macromolecules* **2006**, *38*, 4438-4446.
19. Gardinier, W. E.; Kane, M. A.; Bright, F. V. Effects of Added CO2 on the Dynamics of Poly(dimethylsiloxane) Oligomers Dissolved in a Θ Solvent and a Poor Solvent. *J. Phys. Chem. B* **2004**, *108*, 18520-18529.
20. Kane, M. A.; Pandey, S.; Baker, G. A.; Perez, S. A.; Bukowski, E. J.; Hoth, D. C.; Bright, F. V. Effects of Density on the Intramolecular Hydrogen Bonding, Tail-Tail Cyclization, and Mean-Free Tail-to-Tail Distances of Pyrene End-Labeled

Poly(dimethylsiloxane) Oligomers Dissolved in Supercritical CO2. *Macromolecules* **2001**, *34*, 6831-6838.

21. Winnik, M. A.; Li, X.-B.; Guillet, J. E. Effects of Added Polymer on the Conformation and Dynamics of Polystyrene Containing Evenly Spaced Pyrene Groups. *Macromolecules* **1984**, *17*, 699-702.
22. Redpath, A. E. C.; Winnik, M. A. The Effect of Polymer Concentration on the Slowest Internal Relaxation Mode of a Labeled Polystyrene Chain. *Polymer* **1983**, *24*, 1286-1290.
23. Irondi, K.; Zhang, M.; Duhamel, J. Study of the Semidilute Solutions of Poly(N,N-dimethylacrylamide) by Fluorescence and Its Implications to the Kinetics of Coil-to-Globule Transitions. *J. Phys. Chem. B* **2006**, *110*, 2628-2637.
24. Redpath, A. E. C.; Winnik, M. A. Temperature d Dependence of Excimer Formation Between Pyrenes at the Ends of a Polymer in a Good Solvent. *J. Am. Chem. Soc* **1982**, *104*, 5604-5607.
25. Farinha, J. P. S.; Picarra, S.; Miesel, K.l.; Martinho, J. M.G. Fluorescence Study of the Coil-Globule Transition of a PEO Chain in Toluene. *J. Phys. Chem. B* **2001**, *105*, 10536-10545.
26. Picarra, S.; Duhamel, J.; Fedorov, A.; Martinho, J. M. G. Coil-Globule Transition of Pyrene-Labeled Polystyrene in Cyclohexane: Determination of Polymer Chain Radii by Fluorescence. *J. Phys. Chem. B* **2004**, *108*, 12009-12015.
27. Ingratta, M.; Duhamel, J. Effect of Side-Chain Length on the Side-Chain Dynamics of α–Helical Poly(L-glutamic acid) as Probed by a Fluorescence Blob Model. *J. Phys. Chem. B* **2008**, *112*, 9209-9218.

28. Farhangi, S.; Weiss, H.; Duhamel, J. Effect of Side-Chain Length on the Polymer Chain Dynamics of Poly(alkyl methacrylate)s in Solution. *Macromolecules* **2013**, *46*, 9738-9747.
29. Mathew, A.; Siu, H.; Duhamel, J. A *Blob* Model to Study Chain Folding by Fluorescence. *Macromolecules* **1999**, *32*, 7100-7108.
30. Duhamel, J. Polymer Chain Dynamics in Solution Probed with a Fluorescence Blob Model. *Acc. Chem. Res.* **2006**, *39*, 953-960.
31. Duhamel, J.; Kanagalingam, S.; O'Brien, T.; Ingratta, M. Side-Chain Dynamics of an α–Helical Polypeptide Monitored by Fluorescence. *J. Am. Chem. Soc.* **2003**, *125*, 12810-12822.
32. Chen, S.; Duhamel, J.; Winnik, M. A. Probing End-to-End Cyclization Beyond Willemski and Fixmann. *J. Phys. Chem. B* **2011**, *115*, 3289-3302.
33. Press, W. H.; Flannery, B. P.; Teukolsky, S. A.; Vetterling, W. T. *Numerical Recipes. The Art of Scientific Computing (Fortran Version)*; Cambridge University Press: Cambridge, 1992.
34. Cuniberti, C.; Perico, A. Intramolecular Excimer Formation in Polymers. Pyrene Labelled Poly(vinyl acetate). *Eur. Polym. J.* **1980**, *16*, 887-893.
35. Ingratta, M.; Mathew, M.; Duhamel, J. How Switching the Substituent of a Pyrene Derivative from a Methyl to a Butyl Affects the Fluorescence Response of Polystyrene Randomly Labeled with Pyrene. *Can. J. Chem.* **2010**, *88*, 217-227.
36. Birks, J. B. *Photophysics of Aromatic Molecules*; Wiley: New York, 1970; p 301.

37. Boileau, S.; Mechin, F.; Martinho, J. M.; Winnik, M. A. End-to-End Cyclization of a Pyrene End-Capped Poly(bisphenol A-diethylene glycol carbonate). *Macromolecules* **1989**, *22*, 215-220.

38. Nishiyama, Y.; Mazeau, K.; Morin, M.; Cardoso, M.B.; Chanzy, H.; Purtaux, J.L. Molecular and Crystal Structure of 7-Fold V-Amylose Complexed with 2-Proanol. *Macromolecules* **2010**, *43*, 8628-9636.

Table of Content